45th AIAA/ASME/ASCE/AHS/ASC Structures, Structural Dynamics & Materials Conference
19 - 22 April 2004, Palm Springs, California

AIAA 2004-1606

Constitutive Modeling of Crosslinked Nanotube Materials

G.M. Odegard*, S.J.V. Frankland†, M.N. Herzog‡, T.S. Gates§, C.C. Fay**
NASA Langley Research Center, Hampton, VA 23681

A non-linear, continuum-based constitutive model is developed for carbon nanotube materials in which bundles of aligned carbon nanotubes have varying amounts of crosslinks between the nanotubes. The model accounts for the non-linear elastic constitutive behavior of the material in terms of strain, and is developed using a thermodynamic energy approach. The model is used to examine the effect of the crosslinking on the overall mechanical properties of variations of the crosslinked carbon nanotube material with varying degrees of crosslinking. It is shown that the presence of the crosslinks has significant effects on the mechanical properties of the carbon nanotube materials. An increase in the transverse shear properties is observed when the nanotubes are crosslinked. However, this increase is accompanied by a decrease in axial mechanical properties of the nanotube material upon crosslinking.

I. Introduction

Carbon nanotube (CNT) composite materials have the potential to provide order-of-magnitude increases in stiffness-to-weight and strength-to-weight ratios relative to current materials used for aerospace structural applications. These properties are especially important in the design and development of ultra-light-weight aircraft such as new classes of Unmanned Aerial Vehicles (UAVs), in which the primary requirements are those associated with long-duration, high-altitude flights. To facilitate the development of CNT-based materials for this purpose, constitutive relationships must be developed that predict the bulk mechanical properties of the materials as a function of the molecular structure.

Within the past few years, considerable effort has been expended to synthesize CNT/polymer composites that take advantage of CNT properties by enhancing the load transfer between the CNTs and the adjacent polymer molecules.[1-9] One approach to achieving this is to form chemical bonds between CNTs and adjacent polymer molecules (functionalization). Despite the potential increase in load transfer that follows from functionalization with respect to the load transfer that occurs without the presence of a chemical bond, it has been recently demonstrated that functionalization itself can measurably affect the structure and mechanical properties of CNTs,[10,11] which can, in turn, ultimately alter or perhaps degrade the bulk mechanical properties of CNT/polymer composite materials. As an alternative approach to increasing load transfer efficiency between the CNT and surrounding polymer, NASA Langley Research Center has recently developed a material in which single-walled CNTs are covalently bonded together (crosslinked) with the chemical linking agent 1,3-bis(4-aminophenoxy-4'-benzoyl)benzene (1,3-BABB). In this material, the short, organic linker units allow for direct CNT-to-CNT load transfer, therefore, possibly allowing for improved overall mechanical properties with respect to pure CNT-based materials and CNT/polymer materials in which the CNTs are functionalized to the polymer only. Since it is expected that the bulk mechanical properties in this new class of materials are expected to be affected by intrinsic and sometimes subtle changes in the molecular structure, a multi-scale modeling approach must be developed to allow for accurate design of materials and provide the constitutive relationships necessary for macro-scale analysis methods.

The objective of the present paper is to develop non-linear constitutive models for these crosslinked CNT materials and to examine the influence of crosslink density on the overall, continuum-level elastic properties. Following a brief description of the materials, the equivalent-continuum modeling approach is described in detail.

---

* Staff Scientist, National Institute of Aerospace. Senior Member, AIAA.
† Staff Scientist, National Institute of Aerospace. Member, AIAA.
‡ NRC Research Associate.
§ Senior Materials Research Engineer, Mechanics and Durability Branch. Associate Fellow, AIAA.
** Senior Polymer Scientist, Advanced Materials and Processing Branch.

The approach includes the determination of the molecular structures of the materials using molecular dynamics (MD) simulations, the development of a non-linear elastic, continuum-based constitutive law using a thermodynamic energy technique, and the determination of the equivalent-continuum material parameters via energy equivalence. The constitutive relationships developed in this paper enables the non-linear elastic behavior of the material to be described in terms of applied strain, which is necessary for the full application of MD techniques in the equivalent-continuum modeling approach. Results from these analyses are compared, and the effect of the crosslinking in these materials is discussed in terms of engineering properties.

II. Materials

The constitutive models developed in this study are for four material systems: a bundle of aligned single-walled CNTs with no crosslinks (0% crosslink density), two bundles of aligned single-walled CNTs with finite crosslink densities (0.3% and 0.45%), and the amorphous pure crosslinking material. The crosslink density is defined as the ratio of the number of functionalized carbon atoms in the CNTs (due to crosslinking) to the total number of carbon atoms in the CNTs. All of the CNTs are achiral (10,10) nanotubes with corresponding diameters of 16.9 Å. The crosslinking material is 1,3-bis(4-aminophenoxy-4'-benzoyl)benzene (1,3-BABB) (Fig. 1). The simulated form of 1,3-BABB is modified to replace the $-NH_2$ groups with hydrogens. Figure 2 shows an example of how the CNTs are crosslinked. Details on the processing and characterization of these materials can be found elsewhere.[12]

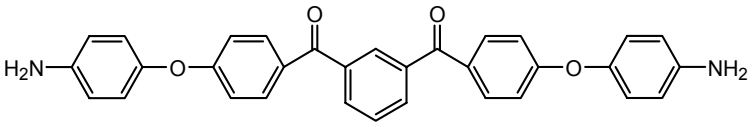

Figure 1. CNT crosslinking material 1,3-BABB

III. Equivalent-Continuum Modeling

The nonlinear-elastic properties of the four materials systems were determined using an equivalent-continuum modeling method.[11,13,14] This approach consisted of three steps. First, representative volume elements (RVE) of the molecular structure and equivalent-continuum models were chosen that accurately described the bulk structure of the material. Next, a constitutive law that described the behavior of the equivalent-continuum model was determined. Finally, the energies of deformation of the two models were equated under identical sets of boundary conditions to determine each of the elastic constants in the constitutive equation. Each of these steps is described in detail below.

A. Representative Volume Element

The RVEs of the molecular and continuum models where selected using the molecular structure of the four materials as a guide. The equilibrium molecular structures of each of the four material systems were determined using MD simulations. The RVE geometry selected was a parallelepiped box. The MD simulation box was then prepared with 9 aligned single-walled CNTs (except for the pure crosslink material) with the proper amount of crosslink material and functionalization sites that corresponded to 0.0%, 0.3%, and 0.45% crosslink densities. The CNTs were aligned parallel to the x_1-axis of the model. Periodic boundary conditions were used in the simulations, thus the CNTs were modeled as having an infinite length. The bonded and non-bonded interactions of the atoms were described by the AMBER force field,[15] without electrostatic interactions. The aromatic rings of the 1,3-BABB were treated as rigid bodies in the simulations. The initial configurations for each of the four systems were compressed using molecular dynamics to minimize the configurational energy, as the size of the simulation box was gradually decreased. An *nPT* (constant number of atoms, pressure, and temperature) algorithm was subsequently applied at a temperature of 298 K and pressure of 1 atm for up to a few picoseconds to establish the equilibrated, undeformed molecular structures. The resulting equilibrium molecular structures are shown in Figs. 3-6. DL-POLY was used for these simulations.[16] Subsequently, the RVE of the continuum models were also formed as solid parallelepipeds with dimensions identical to those of the molecular models, as shown in Figs. 3-6.

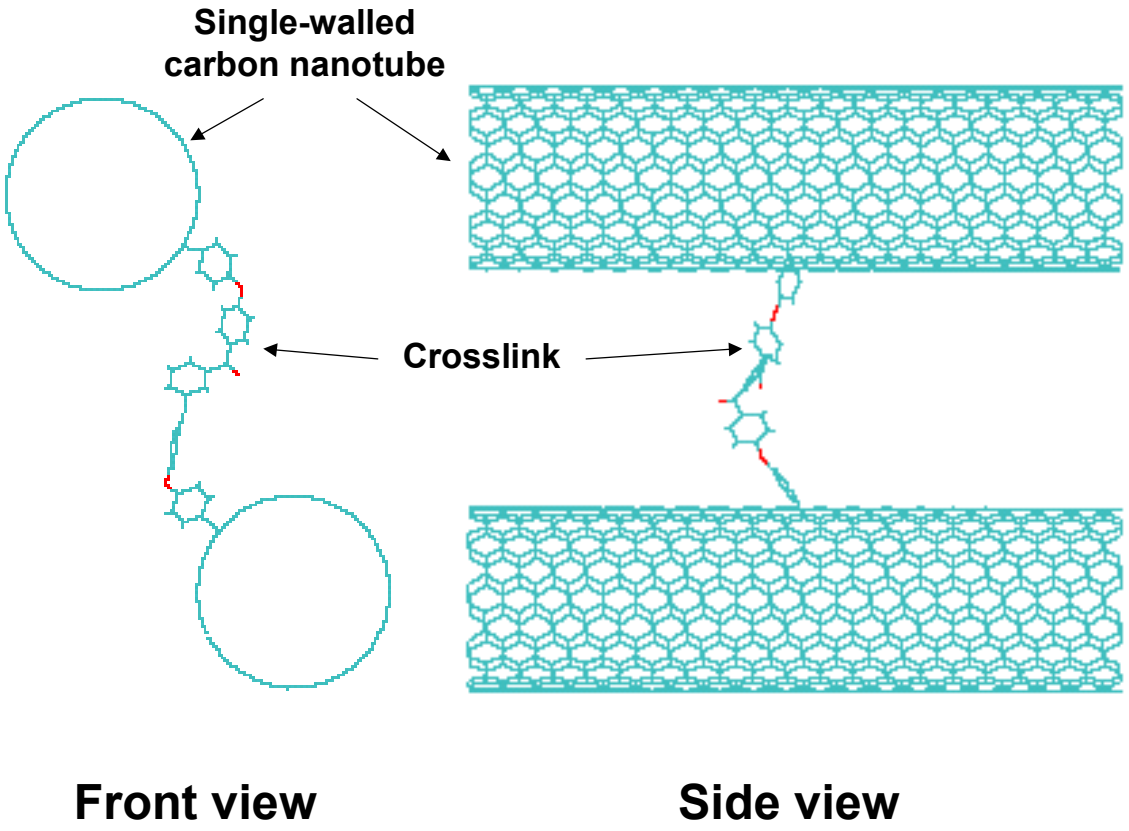

Figure 2. Covalently bonded single-walled CNTs

B. Constitutive Equation

Many materials experience a *nonlinear-elastic* response when subjected to static loads.[17,18] The term *nonlinear-elasticity* can have two different meanings in the description and analysis of material behavior. In the context of this study, the material is nonlinear-elastic in the constitutive sense, not the geometric sense. That is, there is a one-to-one, nonlinear relationship between applied stresses and strains. This study does not consider possible higher-order forms of the stress and strain tensors that reflect the changes in boundary conditions that can occur for large deformations.

A constitutive model that is typically used for nonlinear elastic materials is the Ramberg-Osgood formulation,[19,20] which was originally developed for isotropic materials with the nonlinear term associated with the applied stress. However, because the materials considered in this study are anisotropic, and because it is difficult to apply force-based boundary conditions in MD simulations, an anisotropic, strain-based, nonlinear-elastic constitutive law needed to be established.

Perhaps the most fundamental approach to developing continuum-based constitutive equations for materials is using thermodynamics-based energy functions.[17] This approach allows for the selection of a set of independent variables, such as strain and temperature, that are used to describe overall material behavior through a state function. Since it is necessary for a constitutive law to be expressed in terms of strain when interfacing directly with MD techniques, this thermodynamics-based approach is utilized here to describe the mechanical behavior of crosslinked-CNT materials.

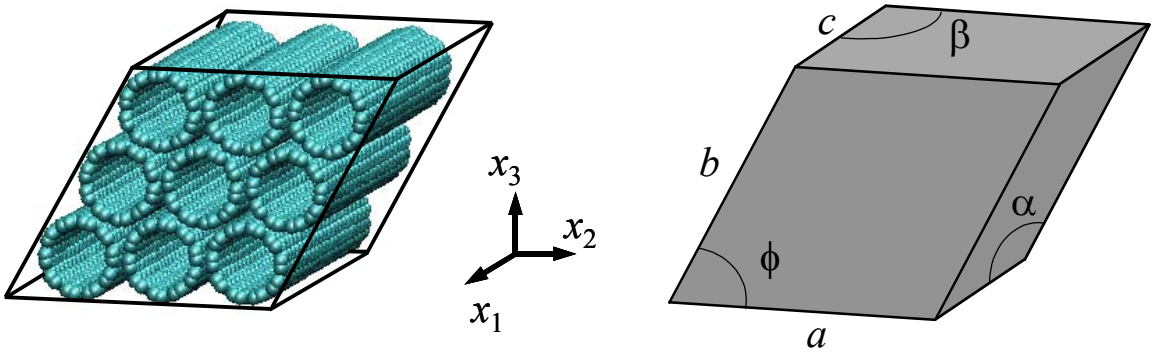

$a = 49.9$ Å $\quad \alpha = 90.0°$
$b = 49.6$ Å $\quad \beta = 90.0°$
$c = 53.8$ Å $\quad \phi = 59.8°$

Figure 3. RVE of CNT bundle with 0% crosslinking

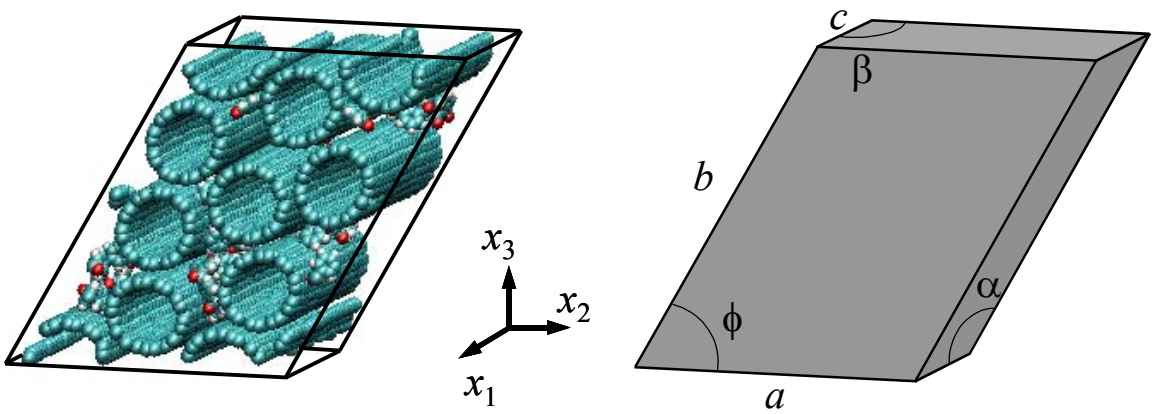

$a = 48.1$ Å $\quad \alpha = 90.0°$
$b = 64.5$ Å $\quad \beta = 90.0°$
$c = 53.8$ Å $\quad \phi = 60.0°$

Figure 4. RVE of CNT bundle with 0.3% crosslinking

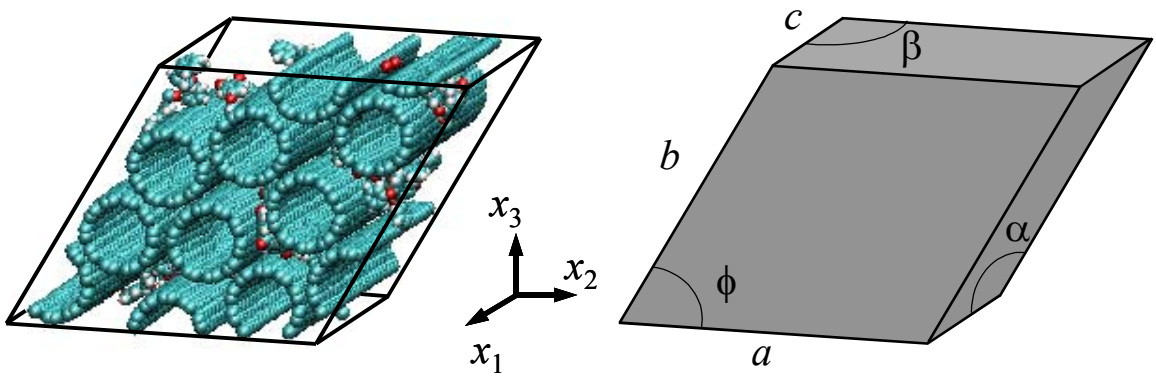

a = 57.5 Å α = 90.0º
b = 56.5 Å β = 90.0º
c = 53.8 Å ϕ = 60.0º

Figure 5. RVE of CNT bundle with 0.45% crosslinking

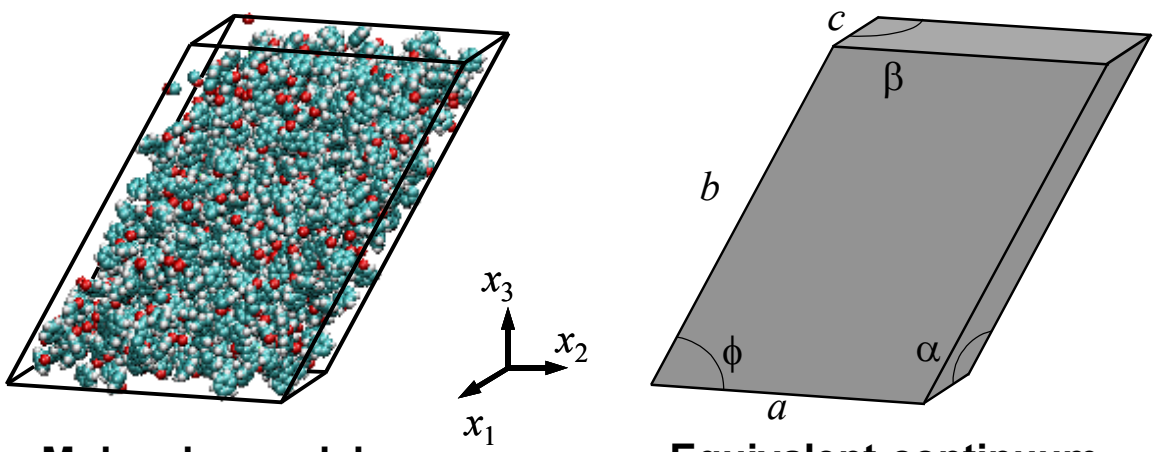

a = 54.2 Å α = 90.0º
b = 86.5 Å β = 90.0º
c = 27.6 Å ϕ = 60.0º

Figure 6. RVE of pure 1,3-BABB crosslinking material

For a uniform, isothermal, homogeneous deformation of a volume of an elastic material, the corresponding uniform stress in the volume is [17]

$$\sigma_{ij} = \frac{1}{V}\frac{\partial F}{\partial \varepsilon_{ij}} \tag{1}$$

where V is the volume of the RVE, ε_{ij} is the strain tensor (i,j = 1,2,3) and F is the Helmholtz free energy, which is henceforth referred to as the strain energy. At this point, it is assumed that the only dependent variables in the strain energy are the applied strains, i.e. $F = F(\varepsilon_{ij})$. The functional form of the strain energy can be further restricted by considering the invariance properties of the material such that the strain energy remains invariant with respect to the coordinate transformations expressed by the material symmetry. Inspection of the molecular models indicates that the constitutive law needs to represent a material with orthotropic symmetry. Therefore, the strain energy must be expressed in terms of the invariants of an orthotropic material, which are [21]

$$\varepsilon_{11}, \varepsilon_{22}, \varepsilon_{33}, \varepsilon_{23}^2, \varepsilon_{13}^2, \varepsilon_{12}^2, \varepsilon_{23}\varepsilon_{13}\varepsilon_{12} \tag{2}$$

For convenience, and because multiples of invariants are also invariants, the strain energy is expressed as

$$\frac{1}{V}F = f\left(\varepsilon_{11}^2, \varepsilon_{22}^2, \varepsilon_{33}^2, \varepsilon_{23}^2, \varepsilon_{13}^2, \varepsilon_{12}^2, \varepsilon_{22}\varepsilon_{33}, \varepsilon_{11}\varepsilon_{33}, \varepsilon_{11}\varepsilon_{22}\right) \tag{3}$$

The functional form of the strain energy is further specified to be sums of individual invariant functions

$$\begin{aligned}\frac{1}{V}F = {} & f_1\left(\varepsilon_{11}^2\right) + f_2\left(\varepsilon_{22}^2\right) + f_3\left(\varepsilon_{33}^2\right) + f_4\left(\varepsilon_{23}^2\right) + f_5\left(\varepsilon_{13}^2\right) + f_6\left(\varepsilon_{12}^2\right) \\ & + f_7\left(\varepsilon_{22}\varepsilon_{33}\right) + f_8\left(\varepsilon_{11}\varepsilon_{33}\right) + f_9\left(\varepsilon_{11}\varepsilon_{22}\right)\end{aligned} \tag{4}$$

where

$$\begin{aligned} f_1\left(\varepsilon_{11}^2\right) &= \frac{1}{n_1+1}A_{11}\left|\varepsilon_{11}^2\right|^{\frac{1}{2}(n_1+1)} \\ f_2\left(\varepsilon_{22}^2\right) &= \frac{1}{n_2+1}A_{22}\left|\varepsilon_{22}^2\right|^{\frac{1}{2}(n_2+1)} \\ f_3\left(\varepsilon_{33}^2\right) &= \frac{1}{n_3+1}A_{33}\left|\varepsilon_{33}^2\right|^{\frac{1}{2}(n_3+1)} \end{aligned} \tag{5}$$

$$\begin{aligned} f_4\left(\varepsilon_{23}^2\right) &= \frac{2^{n_4}}{\left(n_4+1\right)}A_{44}\left|\varepsilon_{23}^2\right|^{\frac{1}{2}(n_4+1)} \\ f_5\left(\varepsilon_{13}^2\right) &= \frac{2^{n_5}}{\left(n_5+1\right)}A_{55}\left|\varepsilon_{13}^2\right|^{\frac{1}{2}(n_5+1)} \\ f_6\left(\varepsilon_{12}^2\right) &= \frac{2^{n_6}}{\left(n_6+1\right)}A_{66}\left|\varepsilon_{12}^2\right|^{\frac{1}{2}(n_6+1)} \end{aligned} \tag{6}$$

$$\begin{aligned} f_7\left(\varepsilon_{22}\varepsilon_{33}\right) &= A_{23}\varepsilon_{22}\varepsilon_{33} \\ f_8\left(\varepsilon_{11}\varepsilon_{33}\right) &= A_{13}\varepsilon_{11}\varepsilon_{33} \\ f_9\left(\varepsilon_{11}\varepsilon_{22}\right) &= A_{12}\varepsilon_{11}\varepsilon_{22} \end{aligned} \tag{7}$$

In Eqns. (5) - (7), n_k (k = 1-6) and A_{ij} are material constants. The power-law relationships in Eqns. (5) and (6) were chosen in order to yield a form of the constitutive relation that would accurately represent the material deformation yet be simple enough to lend itself to the numerical simulations. The constitutive equation that results from Eqns. (1) and (4) - (7) are

$$\begin{aligned}
\sigma_{11} &= A_{11}\varepsilon_{11}^{n_1} + A_{12}\varepsilon_{22} + A_{13}\varepsilon_{33} \\
\sigma_{22} &= A_{12}\varepsilon_{11} + A_{22}\varepsilon_{22}^{n_2} + A_{23}\varepsilon_{33} \\
\sigma_{33} &= A_{13}\varepsilon_{11} + A_{23}\varepsilon_{22} + A_{33}\varepsilon_{33}^{n_3} \\
\sigma_{23} &= A_{44}\gamma_{23}^{n_4} \\
\sigma_{13} &= A_{55}\gamma_{13}^{n_5} \\
\sigma_{12} &= A_{66}\gamma_{12}^{n_6}
\end{aligned} \tag{8}$$

where $\gamma_{ij} = 2\varepsilon_{ij}$. From Eqn. (8) two immediate observations can be made. First, the constants A_{ij} are similar to the elastic stiffness tensor components in linear-elastic materials. Second, all six components of stress exhibit some element of the power-law response with respect to strain. Therefore, it is noted that for a strictly linear elastic material, $n_k = 1$, and for a nonlinear-elastic material, $n_k < 1$. As the material is unloaded, both the strains and stresses will return along the original loading path. Upon full unloading, there will be zero residual deformation.

C. Energy Equivalence

To determine each of the material parameters in Eq. (8), the energies of deformation of the continuum and molecular models were equated for 9 sets of boundary conditions. Each set of boundary conditions corresponded to homogeneous deformations in the continuum models. The displacements applied at the boundaries of the RVE are generalized by

$$u_i(B) = \varepsilon_{ij} x_j \tag{9}$$

where B is the bounding surface of the RVE, x_j is defined in Figs. 3-6, and the summation convention associated with repeated indices is used. The 9 sets of boundary conditions and the material parameters determined for each set are listed in Tables 1-3. The deformations described in Tables 1-3 correspond to axial, plane-strain bulk, and shear deformations, respectively. Unspecified strain components in Tables 1-3 are zero valued.

Table 1. Boundary conditions for axial deformations

Materials parameters	Boundary conditions	Boundary displacements
A_{11}, n_1	$\varepsilon_{11} = e$	$u_1(B) = ex_1$ $u_2(B) = 0$ $u_3(B) = 0$
A_{22}, n_2	$\varepsilon_{22} = e$	$u_1(B) = 0$ $u_2(B) = ex_2$ $u_3(B) = 0$
A_{33}, n_3	$\varepsilon_{33} = e$	$u_1(B) = 0$ $u_2(B) = 0$ $u_3(B) = ex_3$

Table 2. Boundary conditions for plane-strain bulk deformations

Materials parameters	Boundary conditions	Boundary displacements
A_{23}	$\varepsilon_{22} = \varepsilon_{33} = e$	$u_1(B) = 0$ $u_2(B) = ex_2$ $u_3(B) = ex_3$
A_{13}	$\varepsilon_{11} = \varepsilon_{33} = e$	$u_1(B) = ex_1$ $u_2(B) = 0$ $u_3(B) = ex_3$
A_{12}	$\varepsilon_{11} = \varepsilon_{22} = e$	$u_1(B) = ex_1$ $u_2(B) = ex_2$ $u_3(B) = 0$

Table 3. Boundary conditions for shear deformations

Materials parameters	Boundary conditions	Boundary displacements
A_{44}, n_4	$\varepsilon_{23} = \gamma/2$	$u_1(B) = 0$ $u_2(B) = (\gamma/2)x_3$ $u_3(B) = (\gamma/2)x_2$
A_{55}, n_5	$\varepsilon_{13} = \gamma/2$	$u_1(B) = (\gamma/2)x_3$ $u_2(B) = 0$ $u_3(B) = (\gamma/2)x_1$
A_{66}, n_6	$\varepsilon_{12} = \gamma/2$	$u_1(B) = (\gamma/2)x_2$ $u_2(B) = (\gamma/2)x_1$ $u_3(B) = 0$

While the strain energies of the continuum models were determined for each set of boundary conditions using Eqns. (4) - (7), the energies of deformation of the molecular models were determined using MD simulations. For the boundary conditions listed in Tables 1-3, four magnitudes of axial and plane-strain bulk strains were applied; e = 0.5, 1.0, 1.5, and 2.0%; and four magnitudes of shear strains were applied; γ = 0.5, 1.0, 1.5, and 2.0%. For the molecular models, each of the deformations were applied to the equilibrium molecular structures shown in Figs. 3-6 by deforming the MD simulation boxes and all of the atoms in the models according the applied strain field. An *nVT* (constant number of atoms, volume, and temperature) simulation was subsequently used for each deformation to allow the box dimensions to remain fixed while the atoms were allowed to move into new equilibrium positions. The simulations were run up to 2 ps at 298 K using the TINKER modeling package [22] and the AMBER force field [15] without electrostatic interactions. The energy of deformations of the molecular models were averaged over the final 400 fs of each simulation, and the standard error of the energy fluctuations were recorded.

The force field parameters used in the MD simulations are listed in Tables 4-8. In Tables 4-8, R_{min} and E_{min} are the Van der Waals radius and well depth, respectively; K_r and r are the bond-stretching constant and equilibrium distance, respectively; K_θ and θ are the bond-angle constant and equilibrium angle, respectively; and N_{path}, $V_n/2$, γ, and n are the number of bond paths, torsion magnitude, phase offset, and periodicity of the torsion, respectively. Further details of these parameters may be found elsewhere.[15] The carbon atoms in both the CNT and aromatic groups of the crosslinks were modeled as aromatic carbons with sp^2 hybridization, denoted by CA in Table 4 (which is consistent with the AMBER notation). The carbon atoms in the CNTs that were located where the functionalization points exist were modeled as having sp^3 hybridization, denoted as CT in Table 4. The oxygen

atoms in the ether groups of the crosslinks were modeled as having sp^3 hybridization and denoted by OS. The oxygen and carbon atoms in the carboxyl groups of the crosslinks were modeled as having sp^2 hybridization and are denoted by O and C, respectively. The hydrogen atoms on the aromatic groups in the crosslinks are denoted by HA. Fig. 2 shows an example of how the CNTs were crosslinked in the simulations for this phase of the analysis.

With the molecular and equivalent-continuum energies in hand, the next step was to determine the material parameters of Eq. (8). For each set of axial and shear boundary conditions, the computed energies (per unit volume) from the molecular models for all four strain levels were fitted with curves using least squares regression,[23] as a function of the square of the applied strain. The material parameters A_{11}, n_1, A_{22}, n_2, A_{33}, n_3, A_{44}, n_4, A_{55}, n_5, A_{66}, and n_6 were determined for each material using the curve fits and Eqs. (4) - (6). For the plane-strain bulk boundary conditions, the material parameters A_{23}, A_{13}, and A_{12} were determined using the axial parameters A_{11}, n_1, A_{22}, n_2, A_{33}, n_3, and Eqs. (4), (5), and (7). Parameters A_{23}, A_{13}, and A_{12} were adjusted to minimize the correlation coefficient [23] between the energies of the molecular and equivalent-continuum models over the entire applied strain range.

Table 4. Van der Waals parameters

Atom	R_{min} (Å)	E_{min} (kcal/mole)
C	1.9080	0.0860
CA	1.9080	0.0860
CT	1.9080	0.1094
HA	1.4590	0.0150
O	1.6612	0.2100
OS	1.6837	0.1700

Table 5. Bond-stretching parameters

Bond type	K_r (kcal/mole/Å^2)	r (Å)
C-CA	469.0	1.409
C-O	570.0	1.229
CA-CA	469.0	1.400
CA-CT	317.0	1.510
CA-HA	367.0	1.080
CA-OS	320.0	1.410

Table 6. Bond-angle parameters

Bond type	K_θ (kcal/mole/radian^2)	θ (degrees)
CA-C-CA	63.00	120.00
CA-C-O	80.00	120.40
C-CA-CA	63.00	120.00
CA-CA-CA	63.00	120.00
CA-CA-CT	70.00	120.00
CA-CA-HA	35.00	120.00
CA-CA-OS	50.00	109.50
CA-CT-CA	63.00	114.00
CA-OS-CA	60.00	109.50

Table 7. Torsional parameters

Bond type	N_{path}	$V_n/2$ (kcal/mole)	γ (degrees)	n
CA-C-CA-CA	4	14.50	180.0	2.0
CA-C-CA-O	4	14.50	180.0	2.0
C-CA-CA-CA	4	14.50	180.0	2.0
C-CA-CA-HA	4	14.50	180.0	2.0
CA-CA-CA-CA	4	14.50	180.0	2.0
CA-CA-CA-CT	4	14.50	180.0	2.0
CA-CA-CA-HA	4	14.50	180.0	2.0
CA-CA-CA-OS	4	14.50	180.0	2.0
CT-CA-CA-CT	4	14.50	180.0	2.0
CT-CA-CA-HA	4	14.50	180.0	2.0
HA-CA-CA-HA	4	14.50	180.0	2.0
HA-CA-CA-OS	4	14.50	180.0	2.0
CA-CA-CT-CA	6	0.00	0.0	2.0
CA-CA-OS-CA	3	1.15	0.0	3.0

Table 8. Improper torsional parameters

Bond type	N_{path}	$V_n/2$ (kcal/mole)	γ (degrees)	n
CA-CA-CA-CT	1	1.1	180.0	2
CA-CA-CA-HA	1	1.1	180.0	2

IV. Results

The calculated material parameters for all four materials are shown in Table 9. For the CNT bundle systems with and without crosslinking, all of the exponent (n_i) values were 1.0 for the given range of strains (up to 2%) that were applied in the modeling. Thus, for strains under 2%, these systems exhibit linear-elastic behavior. For the same strain range, the 1,3-BABB showed significant nonlinearity under axial deformation, as indicated by the lower values of n_1, n_2, n_3. The 1,3-BABB showed moderate nonlinearity when subjected to shear deformation in the x_2-x_3 plane (n_4).

Table 9. Material parameters (A_{ij} in GPa, n_i is unitless)

Parameter	0% crosslink density	0.3% crosslink density	0.45% crosslink density	1,3-BABB
A_{11}, n_1	570.0, 1.0	440.4, 1.0	463.6, 1.0	0.3, 0.1
A_{22}, n_2	39.5, 1.0	14.3, 1.0	4.2, 1.0	2.7, 0.7
A_{33}, n_3	40.1, 1.0	3.4, 1.0	0.8, 1.0	0.4, 0.1
A_{23}	23.7	4.1	2.1	0.1
A_{13}	9.4	2.8	6.5	0.1
A_{12}	12.1	1.8	5.4	9.0
A_{44}, n_4	1.0, 1.0	28.8, 1.0	22.1, 1.0	12.0, 0.9
A_{55}, n_5	32.1, 1.0	27.7, 1.0	36.5, 1.0	5.3, 1.0
A_{66}, n_6	38.8, 1.0	36.4, 1.0	33.8, 1.0	9.8, 1.0

From Table 9, the effects of the crosslinking on the mechanical properties of the CNT bundles can be discerned. For A_{11}, the stiffness parameter in the nanotube axial direction, a reduction of 23% occurred when the CNTs were crosslinked at a crosslink density of 0.3 %. Little change in A_{11} was observed upon further crosslinking to a crosslink density of 0.45%. More significant losses were sustained by the transverse stiffness parameters A_{22}, and A_{33}, with reductions of up to 92% at a crosslink density of 0.3%. Furthermore, A_{22} and A_{33} continued to decrease significantly upon further crosslinking to a crosslink density of 0.45%. For A_{33}, a total loss of 98% occurred between the non-crosslinked and the 0.45% crosslinked systems. Therefore, it is clear that the crosslinking of the CNTs degrades the mechanical properties of the CNT bundles when these bundles are deformed parallel to the principle axes of the material (Figs. 3-6).

The material response to plane-strain bulk deformations is evident by noting the calculated values in Table 9. The transverse plane-strain bulk deformation parameter, A_{23}, decreased by 83% and 91% for the 0.3% and 0.45%

crosslink densities, respectively. The longitudinal plane-strain bulk parameters, A_{13} and A_{12}, decreased significantly (up to 85%) when the CNTs were crosslinked to a density of 0.3%. However, the same parameters increased (up to a factor of 3) upon further crosslinking up to 0.45%. Therefore, while the parameter A_{23} shows a clear degradation upon CNT crosslinking, there was no clear effect of crosslinking on the parameters A_{13} and A_{12}.

The effects of crosslinking on the shear moduli are also evident from the data in Table 9. Under a transverse shear load, the resulting mechanical parameter, A_{44}, increased by a factor of 29 when the CNTs were crosslinked up to 0.3%. Little change was observed under the same loading condition upon further crosslinking. The response to longitudinal deformation (A_{55}, A_{66}) was not significantly affected by the crosslinking in the bundle systems. Therefore, the crosslinking of the CNT enhanced the transverse shear properties while having little effect on the longitudinal shear properties.

For completeness, the stiffness parameters for the pure crosslinking material 1,3-BABB are also included in Table 9. As expected for an organic molecular solid, the pure material had relatively low mechanical properties compared with the CNT materials. In particular, the axial mechanical parameters A_{11}, A_{22}, A_{33}, n_1, n_2, and n_3; the longitudinal shear parameters A_{55} and A_{66}; and the plane strain bulk parameters A_{23} and A_{13} were significantly smaller for the 1,3-BABB than those of all three of the CNT systems.

V. Summary

In this study, a nonlinear constitutive model was developed for CNT-bundle materials in which the CNTs had varying amounts of crosslink densities. An equivalent-continuum modeling approach was used to develop the continuum-based, non-linear elastic constitutive relationship that incorporated the subtle changes in molecular structure upon crosslinking. In the equivalent-continuum modeling, MD simulations were performed to determine the equilibrium molecular structure of these systems as well as to determine the molecular structure and corresponding energy changes when subjected to applied strains. As a result, the effects of material nonlinearity and the influence of the crosslinking on the mechanical properties of the CNT materials were discerned.

Even though the CNT materials did not exhibit any nonlinear behavior, the pure crosslinking material was nonlinear, as indicated by the lower values of the power-law exponents in the constitutive equation. Overall, the presence of the crosslinks had significant effects on the mechanical properties of the CNT bundles. In particular, the crosslinks degraded the axial mechanical properties and the transverse plane-strain bulk properties of the CNT bundles. A decrease of up to 98% and 91% was observed for the axial and transverse plane-strain bulk parameters, respectively, when a 0.45% crosslink density was applied to CNT bundles. However, the crosslinking greatly enhanced the transverse shear properties. A nearly 30-fold increase was observed for the transverse shear parameter between the non-crosslinked and 0.3% crosslink density systems.

References

[1]Chen, R.J.; Zhang, Y.; Wang, D., and Dai, H., "Noncovalent Sidewall Functionalization of Single-Walled Carbon Nanotubes for Protein Immobilization," *Journal of the American Chemical Society*, Vol. 123, 2001, pp. 3838-3839.

[2]Star, A.; Stoddart, J.F.; Steuerman, D.; Diehl, M.; Boukai, A.; Wong, E.W.; Yang, X.; Chung, S.; Choi, H., and Heath, J.R., "Preparation and Properties of Polymer-Wrapped Single-Walled Carbon Nanotubes," *Angewandte Chemie International Edition in English*, Vol. 40, No. 9, 2001, pp. 1721-1725.

[3]Lordi, V. and Yao, N., "Molecular Mechanics of Binding in Carbon-Nanotube-Polymer Composites," *Journal of Materials Research*, Vol. 15, 2000, pp. 2770-2779.

[4]Jia, Z.; Wang, Z.; Xu, C.; Liang, J.; Wei, B.; Wu, D., and Zhu, S., "Study on Poly(Methyl Methacrylate)/Carbon Nanotube Composites," *Materials Science and Engineering A*, Vol. A271, 1999, pp. 395-400.

[5]Wagner, H.D.; Lourie, O.; Feldman, Y., and Tenne, R., "Stress-Induced Fragmentation of Multiwall Carbon Nanotubes in a Polymer Matrix," *Applied Physics Letters*, Vol. 72, 1998, pp. 188-190.

[6]Chen, J.; Hamon, M.A.; Hu, H.; Chen, Y.; Rao, A.M.; Eklund, P.C., and Haddon, R.C., "Solutions Properties of Single-Walled Carbon Nanotubes," *Science*, Vol. 282, 1998, pp. 95-98.

[7]Michelson, E.T.; Huffman, C.B.; Rinzler, A.G.; Smalley, R.E.; Hauge, R.H., and Margrave, J.L., "Fluorination of Buckytubes," *Chemical Physics Letters*, Vol. 296, 1998, pp. 188-194.

[8]Boul, P.J.; Liu, J.; Michelson, E.T.; Huffman, C.B.; Ericson, L.M.; Chiang, I.W.; Smith, K.A.; Colbert, D.T.; Hauge, R.H.; Margrave, J.L., and Smalley, R.E., "Reversible Sidewall Functionalization of Buckytubes," *Chemical Physics Letters*, Vol. 310, 1999, pp. 367-372.

[9]Frankland, S.J.V.; Caglar, A.; Brenner, D.W., and Griebel, M., "Molecular Simulation of the Influence of Chemical Cross-Links on the Shear Strength of Carbon nanotube-Polymer Interfaces," *Journal of Physical Chemistry B*, Vol. 106, 2002, pp. 3046-3048.

[10]Frankland, S.J.V.; Odegard, G.M., and Gates, T.S., "The Effect of Functionalization on Double-Walled Nanotube Materials," *International Symposium on Clusters and Nano-Assemblies: Physical and Biological Systems*. 2003.

[11]Odegard, G.M.; Frankland, S.J.V., and Gates, T.S., "The Effect of Chemical Functionalization on Mechanical Properties of Nanotube/Polymer Composites, AIAA 2003-1701," *44th AIAA/ASME/ASCE/AHS/ASC Structures, Structural Dynamics, and Materials Conference*. 2003.

[12]Frankland, S.J.V.; Herzog, M.N.; Odegard, G.M.; Gates, T.S., and Fay, C.C., "Modeling and Characterization of Elastic Constants of Functionalized Nanotube Materials," *Materials Research Society Symposium Proceedings*, 2003. Vol. 791, Q9.10:1-6.

[13]Odegard, G.M.; Gates, T.S.; Nicholson, L.M., and Wise, K.E., "Equivalent-Continuum Modeling of Nano-Structured Materials," *Composites Science and Technology*, Vol. 62, No. 14, 2002, pp. 1869-1880.

[14]Odegard, G.M.; Gates, T.S.; Wise, K.E.; Park, C., and Siochi, E.J., "Constitutive Modeling of Nanotube-Reinforced Polymer Composites," *Composites Science and Technology*, Vol. 63, 2003, pp. 1671-1687.

[15]Cornell, W.D.; Cieplak, P.; Bayly, C.I.; Gould, I.R.; Merz, K.M.; Ferguson, D.M.; Spellmeyer, D.C.; Fox, T.; Caldwell, J.W., and Kollman, P.A., "A Second Generation Force Field for the Simulation of Proteins, Nucleic Acids, and Organic Molecules," *Journal of the American Chemical Society*, Vol. 117, 1995, pp. 5179-5197.

[16]Smith, W. and Forester, T.R., DL-POLY, Warrington, England, The Council for the Central Laboratory of the Research Councils, 1996.

[17]Fung, Y.C., *Foundations of Solid Mechanics*, Prentice-Hall, Inc., Englewood Cliffs, NJ, 1965.

[18]Ashby, M.F. and Jones, D.R.H., *Engineering Materials 1: An Introduction to Their Properties and Applications*, Butterworth-Heinemann, Oxford, 1996.

[19]Ramberg, W. and Osgood, W.R., "Description of Stress-Strain Curves by Three Parameters," NACA Technical Notes No. 902, 1943.

[20]Hutchinson, J.W., "Fundamentals of the Phenomonological Theory of Nonlinear Fracture Mechanics," *Journal of Applied Mechanics*, Vol. 50, 1983, pp. 1042-1051.

[21]Spencer, A.J.M., "Theory of Invariants," *Continuum Physics: Volume 1-Mathematics*. Academic Press, New York, 1971, pp. 239-353.

[22]Ponder, J.W., TINKER: Software Tools for Molecular Design, Ver. 3.8, Washington University School of Medicine, 1998.

[23]Press, W.H.; Flannery, B.P.; Teukolsky, S.A., and Vetterling, W.T., *Numerical Recipes*, Cambridge University Press, Cambridge, 1986.